Am J Transl Res 2016;8(12):5199-5210
www.ajtr.org /ISSN:1943-8141/AJTR0033646

Original Article

NADPH oxidase activation played a critical role in the oxidative stress process in stable coronary artery disease

Jiefang Zhang[1,2], Meihui Wang[2], Zhengwei Li[1], Xukun Bi[1], Jiale Song[1], Shaoxiang Weng[2], Guosheng Fu[1,2]

[1]*Department of Cardiology, Sir Run Run Shaw Hospital, College of Medicine, Zhejiang University, Zhejiang, China;* [2]*Biomedical Research (Therapy) Center, Sir Run Run Shaw Hospital, Hangzhou, Zhejiang, China*

Received June 13, 2016; Accepted October 30, 2016; Epub December 15, 2016; Published December 30, 2016

Abstract: Objectives: The study was designed to investigate the oxidative stress levels of endothelial progenitor cells (EPCs) in stable coronary artery disease (CAD) and to explore the underlying mechanisms of NADPH oxidase activation and subsequent EPCs dysfunction. Methods: EPCs were isolated from patients with stable CAD (n=50) and matched healthy volunteers (n=50). NADPH oxidase activation was detected by measuring the expression of each subunit using western blotting and qPCR analyses and the membrane translocation of $p47^{phox}$ using immunofluorescence. The in vivo angiogenesis capacity was evaluated using immunofluorescence by transplanting EPCs into a rat hind limb ischemia model. The PKC inhibitor GÖ-6983 was used to determine the role of PKC in NADPH oxidase activation. Results: Oxidative stress level was increased and the in vivo angiogenesis capacity was impaired in EPCs obtained from CAD subjects with the activation of NADPH oxidase. $P47^{phox}$ membrane translocation increased in CAD group vs controls. These effects were resolved by NADPH oxidase inhibition. Up-regulation of PKCα/β2 was found in EPCs from CAD subjects, PKC inhibition GÖ-6983 could reduce the expression and activity of NADPH oxidation. Conclusions: NADPH oxidase activation via $p47^{phox}$ membrane translocation played a critical role in the initiation and progression of CAD, and the PKCα/β2 signaling pathway might be involved.

Keywords: NADPH oxidase, reactive oxygen species, stable coronary artery disease, endothelial progenitor cells, PKC

Introduction

It has been suggested that EPCs might not only be responsible for the recovery of the endothelium after injury but also contribute to angiogenesis, providing the hope of new treatment opportunities [1]. Indeed, there is accumulating evidence demonstrating a reduction in the number of EPCs and impaired EPC function in the presence of cardiovascular disease [2]. The most important mechanism is the diverse reactive oxygen species (ROS) produced at increased levels [3]. Excessive ROS production severely impaired EPC mobilization, migration and proliferation, as well as its vasculogenic capacity. However, the specific mechanism is not completely clear. In stem/progenitor cells, ROS is mainly derived from NADPH oxidase [4]. Previous studies have shown that in EPCs obtained from diabetes, NADPH oxidase activation via $p47^{phox}$ membrane translocation and binding to the subunit Nox2 or Nox4 can cause increased production of ROS, decreased nitric oxide (NO) bioactivity and re-endothelialization dysfunction [5]. However, in EPCs derived from CAD, the effects of NADPH oxidase activation on the vasculogenic capability remain unknown.

In addition, there is increasing evidence that PKC activation is important in diabetes-related endothelial dysfunction and in the activities of receptors mediating smooth muscle contraction via activation of NADPH oxidase [6]. However, only minimal attention has been given to defining the role of PKC systems in the activation of NADPH oxidases. In EPCs derived from CAD, whether NADPH oxidase activation is mediated via the PKC signaling pathway has not been elucidated to date.

The current study aimed to explore the NADPH oxidase activation process and its underlying

Table 1. Baseline characteristics

Characteristics	Coronary heart disease (N=50)	Control subjects (N=50)	*P* value
Age, y	58.9 ± 5.7	60.5 ± 5.4	NS
Sex, % men	64	59	NS
Smokers, %	35	31	NS
Hypertension, %	60	57	NS
Diabetes, %	0	0	NS
Cholesterol (total), mg/dL	194 ± 56	167 ± 40	P>0.05
Triglycerides, mg/dL	162 ± 69	150 ± 47	P>0.1
Severity (1/2/3 vessel disease), %	67, 26, 7	0	
History of taking statin, %	0	0	NS

Note: Values are percentages or mean ± SD.

Table 2. List of primers used in qRT-PCR

	Sense primers (5'-3')	Antisense primers (5'-3')
$gp91^{phox}$	TACCTGGCTGTGACCCTGTT	GGTTTTGGTGGAGGAAGTGA
$p47^{phox}$	ACGAGACGGAAGACCCTGAG	GACGGGAAGTAGCCTGTGAC
$p22^{phox}$	GTACTTTGGTGCCTACTCCA	CGGCCCGAACATAGTAATTC
Nox4	CAGGAGGGCTGCTGAAGTATCAA	TGACTGGCTTATTGCTCGGATA
GAPDH	GGGTGTGA CCATGAGAAGT	GACTGTGGTCATGAGTCCT

mechanisms, as well as the changes in the vasculogenic capacity resulting from NADPH oxidase activation in EPCs from CAD.

Materials and methods

Characteristics of the patients and controls

Fifty stable CAD patients were consecutively enrolled. The control group consisted of fifty volunteers who were matched for gender and age with the CAD patients, a clinical evaluation was performed to ensure the healthy status of the control subjects. The clinical details of the studied population are shown in **Table 1**. The diagnosis of stable CAD was based on clinical assessment, echocardiography, and angiography. Patients who fulfilled the following inclusion criteria were enrolled in the study: previously diagnosed CAD without angina, or symptom complex that has remained stable for at least 60 days (No change in frequency, duration, precipitating causes or ease of relief of angina for at least 60 days); And no evidence of recent myocardial damage; Percutaneous coronary intervention (PCI) in 1 or 2 or 3 major coronary arteries. Exclusion criteria were previous coronary bypass surgery, significant coronary artery disease in all the major epicardial coronary arteries or left main coronary stenosis ≥50%, unstable angina, and acute myocardial infarction. All patients and controls had no diabetes and were free of wounds, ulcers, retinopathy, recent surgery, inflammatory, malignant diseases and acute coronary syndrome (ACS). All the subjects were in accord with the ethical standards established by the Human Research Protections (OHRP). Informed consent was obtained from all subjects, and all of the procedures were performed according with national and international laws and policies.

EPC cultures and identification of late-EPCs

EPCs were isolated, cultured and characterized according to previously described techniques [7]. Briefly, mononuclear cells (MNCs) were isolated from the peripheral blood of patients or control subjects using Ficoll density gradient centrifugation and were plated onto six-well plates coated with human fibronectin (Chemicon, USA) and maintained in endothelial basal medium (EBM)-2 (Clonetics, Lonza, USA) supplemented with 10% fetal-calf serum (FBS) (Gibco, Invitrogen, USA), and other cytokines. After 48 h in culture, non-adherent cells were removed and re-plated onto six-well plates. The culture was maintained for seven days to obtain the colony-forming unit endothelial cells (CFU-EC). Adherent cells were cultured for 2-4 weeks to obtain late endothelial progenitor cells (L-EPCs). L-EPCs were incubated with 1,1-dioctadecyl-3,3,3,3-tetramethylindocarbocyanine (DiI)-labeled acetylated low-density lipoprotein (acLDL; Molecular Probe) and stained with FITC-labeled Ulex europaeus agglutinin (UEA-1; Sigma). After staining, the samples were visualized using a laser scanning confocal microscope (LSCM, Leica). Cells demonstrating double-positive fluorescence were identified as L-EPCs. Moreover, they were shown to express KDR, CD34 (Becton Dickinson, USA) and AC133

(Miltenyi Biotec, Germany) using flow cytometry (Supplementary Figures 1, 2 and 3).

ROS measurement

EPCs were incubated in EGM2 with 10 μM 2',7'-dichlorodihydrofluorescein diacetate (H2-DCF-DA) (Molecular Probes) for 1 h at 37°C in the dark. Next, the cells were trypsinized and washed three times with PBS before the reaction was terminated. The Mean Fluorescence Intensity (MFI) of the cells were measured using FACS analysis. No fluorescent probe samples served as the negative control [8].

Measurement of NADPH oxidase activity

The NADPH oxidase activity was measured using the lucigenin-enhanced chemiluminescent detection of superoxide anions [9]. The EPC lysates were mixed with phosphate buffer (50 mM, pH 7.0) containing ethylene glycol tetraacetic acid (EGTA, 1 mM), sucrose (150 mM), lucigenin (the electron acceptor, 5 μM) and NADPH (the substrate, 100 μM). Photon emission was measured every 2 minutes for 4 times using a chemiluminescence analyzer (Biotek, USA).

Malondialdehyde (MDA) assay

The medium was removed and the EPCs were gently washed with ice-cold PBS three times and lysed in cell lysis buffer. The lysate was centrifuged at 10,000×g for 5 min. The supernatant was used to evaluate lipid peroxidation, which was determined using a lipid peroxidation MDA assay kit (Beyotime Co., Shanghai, China) [10].

Quantitative RT-PCR

Total RNA was extracted using TRIzol (Invitrogen, Carlsbad, CA, USA). cDNA synthesis was performed with 1 μg of total RNA using the miScript II RT Kit (Qiagen, Germany) according to the manufacturer's instructions. Sequences of the primers sequences can be found in **Table 2**. Real-time PCR was performed on the ABI 7500 cycler (Applied Biosystems, CA, USA), using the miScript SYBR Green PCR Kit (Qiagen, Germany) according to the manufacturer's protocol. Glyceraldehyde-3-phosphate dehydrogenase (GAPDH) was used as an endogenous control for mRNA expression.

Western blotting analyses and antibodies

EPCs were scraped in RIPA lysis buffer (Beyotime, Shanghai, China) that was supplemented with 1 mM PMSF. The primary antibodies used in the current study included Anti-$p22^{phox}$, anti-Nox4, anti-pPKCα/β1/β2 were purchased from Cell Signaling Technology (Beverly, MA, USA). Anti-$gp91^{phox}$ and anti-$p47^{phox}$ were purchased from Abcam Ltd. (MA, USA). Anti-GAPDH polyclonal antibody was purchased from Santa Cruz Biotechnology (CA, USA). Secondary antibodies conjugated to horseradish peroxidase were purchased from Cell Signaling Technology. The images were captured on the image reader LAS-4000 system (Fujifilm, Tokyo, Japan).

Small-interfering RNA transfection

NADPH oxidase subunit expression were silenced with the use of Validated Stealth RNAi (Invitrogen, Carlsbad, Calif), siRNA transfection was carried out according to the manufacturer's protocol. The small-interfering RNA (siRNA) sequences (sense strands) used for targeting human $p47^{phox}$ were 5'-CGGAGAGACGAGUAUAACCCAGUUU-3', for targeting Nox2 were 5'-GGCUGUGCAUAAUAUAACATT-3', for targeting Nox4 were GGCAGGAGAACCAGGAGAUUTT-3'. In brief, EPCs were transferred into 6-well plates and cultured in EM2 supplemented with 20% FBS. After overnight growth, the cells at 80% adherence were treated with 0.5 ml of Opti-MEM I (Invitrogen, Canada) with each well containing 50 nmol/l siRNA duplexes and 5 μl of Lipofectamine2000. In addition, an RNAi Negative Control Duplex was used as a negative control. All siRNA transfections were performed for 24 hours preceding subsequent EPCs measurements.

Mobilization of $p47^{phox}$ subunits to the plasma membrane

Translocation of $p47^{phox}$ subunits to the membrane was analyzed using immunofluorescence [11]. Briefly, the cells were cultured on coverslips and permeabilized by incubating for 15 minutes on ice with 2 ml of 0.1% Triton X-100 in PBS. After incubating for 1 hour with blocking buffer (DAKO) (Abcam Ltd., MA, USA), $p47^{phox}$ primary antibodies (9.4 μg/ml) were introduced to the sample and incubated at 4°C overnight. The cells were washed with PBS for 5 minutes

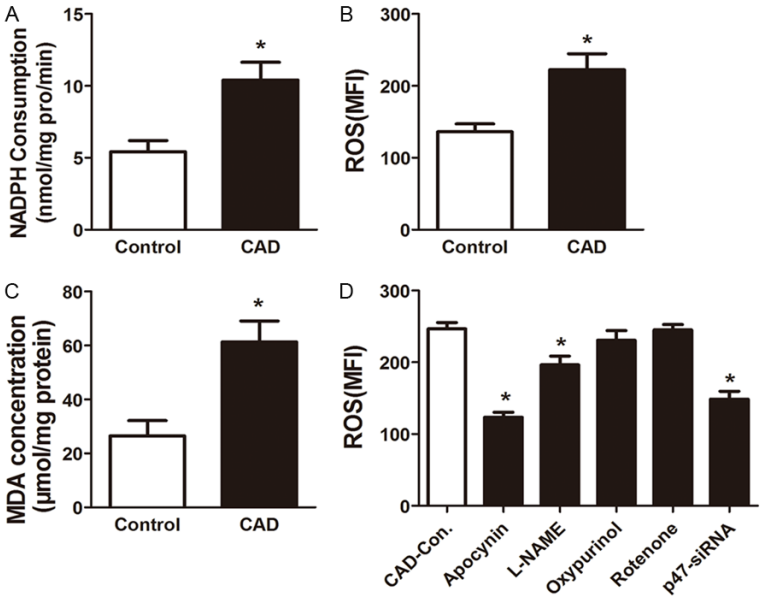

Figure 1. NADPH oxidative activity, ROS and MDA levels in two groups. A. NADPH consumption were enhanced from 5.4 to 10.4 nmol/mg protein/min in EPCs from CAD versus control groups, *n*=11, 12, **P<0.05.* B. ROS production were significantly increased by 63.5% in EPCs from CAD versus control groups, *n*=13, 15, **P*<0.05. C. The concentrations of MDA were elevated by 131% in EPCs from CAD subjects versus control groups, *n*=14, 17, **P*<0.05. D. The main source of ROS in CAD-EPCs. EPCs from CAD subjects were incubated with apocynin (100 μmol/L), L-NAME (1 mmol/L), oxypurinol (100 μmol/L), rotenone (250 μmol/L) and $p47^{phox}$ siRNA, EPCs from CAD subjects without intervention were used as the control group, *n*=6 per group. ROS production was significantly reduced in the group of apocynin, L-NAME and $p47^{phox}$ siRNA (**P*<0.05).

and repeated five times. The cells were incubated in fluorescein-conjugated secondary antibodies (DyLight 594 AffiniPure Goat Anti-Rat IgG) in blocking buffer in a dark humidity chamber at 4°C for 1 hour. After several washes with PBS, the samples were detected using a fluorescence microscope.

Animals and in vivo vasculogenic capacity assay

Twenty male Sprague-Dawley rats weighing 200-220 g (from Zhejiang University experimental animal center) were randomly divided into a control group and a CAD group (n=10 for each group). All procedures were performed according to the Guide of Zhejiang University Animal Care and Use Committee, and approval was granted by the university ethics review board. A rat hind limb ischemia model was generated by a femoral artery ligation. SD rats were anesthetized with intraperitoneal injection of 8% chloral hydrate (0.5 ml/100 g). Saline, control group EPCs and CAD EPCs labeled with DiI (1,1'-dioctadecyl-3,3,3',3'-tetramethylindocarbocyanine perchlorate) were injected into the ipsilateral gastrocnemius. Laser Doppler Flowmetry PeriFlux 5000 (Perimed, Sweden) was used for the blood flow measurements. An optic probe was positioned and fixed at a right angle above the medial side of the ligated limb. By receiving the optical fiber, the information is recorded and converted into electrical signals for analysis. Measurements of PU (Perfusion Unit) were obtained before the occlusion, immediately after the transplantation, and 15 d, 28 d after transplantation. The data were analyzed using PeriFlux 5000-PC-Software.

Transplanted EPCs to participate in angiogenesis of new blood vessels were evaluated by immunofluorescence. 28 days after transplantation, the gastrocnemius muscle tissue from the hind limb ischemia model of both the CAD/control subjects were fixed in 4% formalin and was embedded in paraffin. Sections were stained with FITC-labeled lectin griffonia simplicifolia (Sigma, USA) and 4,6-diamino-2-phenyl indole (DAPI). Homing of the transplanted EPCs to the site of vascular injury were detected using fluorescence microscopy. The mean values of the neovascularization numbers were used for the analysis [5].

Statistical analysis

All experiments were performed at least three times. All data were presented as mean ± standard deviation (SD). Two groups were compared using t-test comparison and One way analysis of variance (ANOVA) with a one-tailed Student's t-test was used for multiple comparisons among groups. Statistical analysis was done with SPSS version 18.0. *P*-values <0.05 were considered statistically significant.

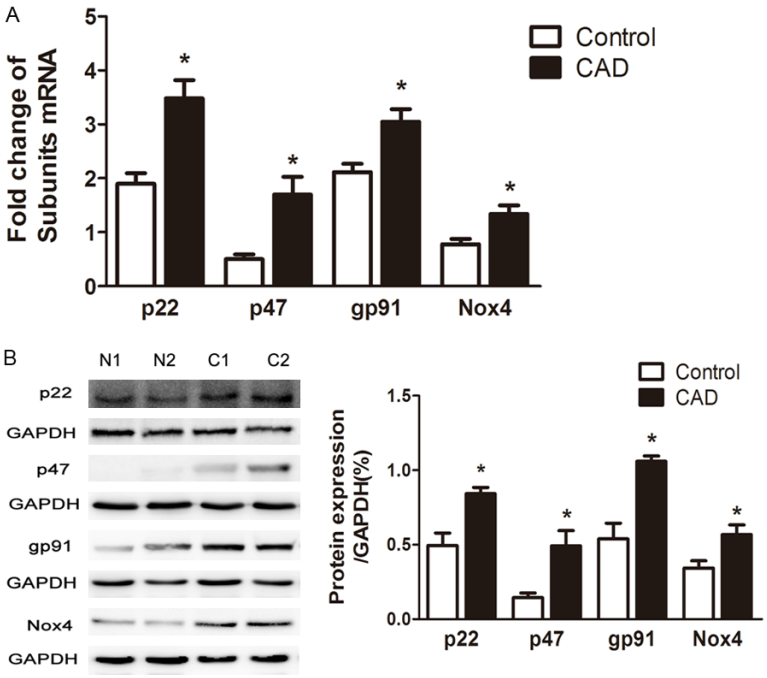

Figure 2. The mRNA and protein expression of NADPH oxidase subunit levels in CAD and control groups, *n*=8, 8. A. Fold changes of $p22^{phox}$, $p47^{phox}$, $gp91^{phox}$ and Nox4 subunits mRNA were significantly increased in CAD group versus controls, **P*<0.05. B. Protein expression of $gp91^{phox}$, $p22^{phox}$ and $p47^{phox}$ were increased in CAD group (C1, C2) versus controls (N1, N2), **P*<0.05.

Results

NADPH oxidase activity, ROS production and MDA levels

We evaluated the NADPH oxidase activity, ROS and MDA levels in EPCs from CAD subjects and normal control as described above. These results showed that NADPH consumption was enhanced from 5.4 to 10.4 nmol/mg protein/min (P<0.05), the ROS levels were significantly increased by 63.5% in EPCs from CAD (P<0.05). Concentrations of MDA were elevated by 131% in EPCs from CAD subjects (P<0.05) (**Figure 1**). All of these indicated that the oxidative stress levels of EPCs in stable coronary artery disease were significantly increased.

Increased expression of NADPH oxidase subunits

The mRNA expression of NADPH oxidase subunits were detected using qPCR. These results indicated that the mRNA expression of $p22^{phox}$, $p47^{phox}$, $gp91^{phox}$ and Nox4 significantly increased in EPCs from CAD group (P<0.05). In addition, the protein expression of subunits were detected using western blotting analyses, and showed the expression of $p22^{phox}$, $p47^{phox}$, $gp91^{phox}$ and Nox4 were increased consistently in EPCs from CAD subjects (**Figure 2**).

$p47^{phox}$ membrane translocation

The translocation of $p47^{phox}$ subunits of NADPH oxidase from the cytosol to the plasma membrane is an essential step in the activation of NADPH oxidase. $p47^{phox}$ positioning within EPCs was analyzed using indirect immunofluorescence. Anti-$p47^{phox}$ was labeled with Dyl594 fluorescent secondary antibody (red), and the nuclei were stained with DAPI (blue). In control group, $p47^{phox}$ was evenly distributed in the cell. However, in CAD group, $p47^{phox}$ translocated from the cytoplasm to the plasma membrane, demonstrating uneven distribution, with enhanced distribution of the inner membrane and weaker cytoplasmic distribution, which reflected activation of $p47^{phox}$ in EPCs from CAD (**Figure 3A**, **3B**). Calculating the cell numbers which $p47^{phox}$ was activated per unit area in EPCs, we can evaluate the $p47^{phox}$ activation rate in each groups. $p47^{phox}$ activation rate was 31.6% in the CAD group, while 17.8% in control group , activation rate in CAD was 1.78 times higher compared to the control group, N=10, 10, *P<0.05 (**Figure 3C**).

In vivo angiogenesis capacity of EPCs was severely impaired in CAD subjects

We evaluated EPC angiogenesis in vivo by transplanting EPCs into a rat hind limb ischemia model as described above. Prior to the operative ligation of the femoral artery, hind limb perfusion of the rats was not impaired and the base flow were nearly the same in the CAD and control group (n=10, 10). After occlusion, two groups of rats received a local injection of 1×10^5 transduced EPCs (control-EPCs, and CAD-EPCs). Examination of the hind limb perfu-

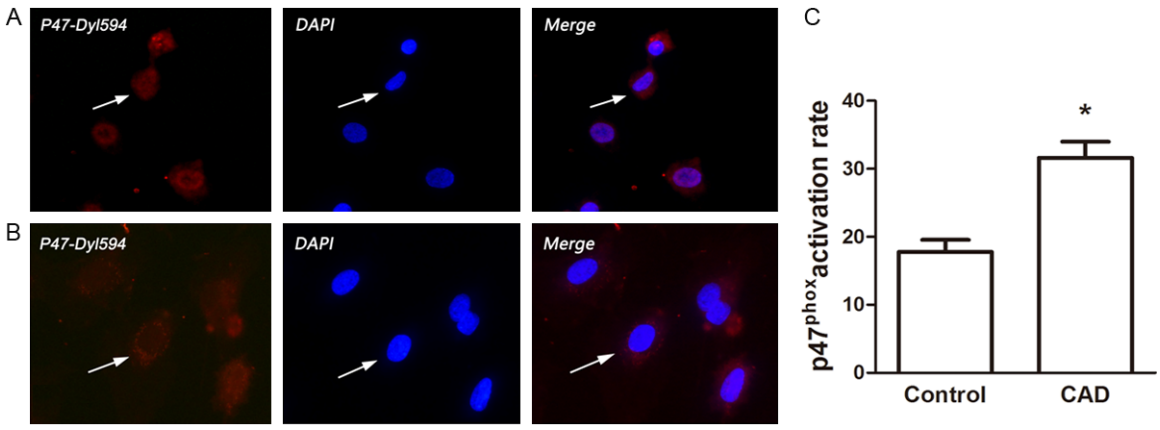

Figure 3. Immunofluorescence of p47^{phox} membrane translocation. Anti-p47^{phox} was labeled with Dyl594 fluorescent secondary antibody (red), and the nuclei were stained with DAPI (blue). A. In control group, p47^{phox} was evenly distributed in the cell (arrow). B. In CAD group, p47^{phox} translocated from the cytoplasm to the plasma membrane, demonstrating uneven distribution, with enhanced distribution of the inner membrane and weaker cytoplasmic distribution (arrow) (×400). C. Statistical graph of p47^{phox} activation rate. p47^{phox} activation rate was 31.6% in the CAD group, while 17.8% in control group , activation rate in CAD was 1.78 times higher compared to the control group, n=10, 10, *P<0.05.

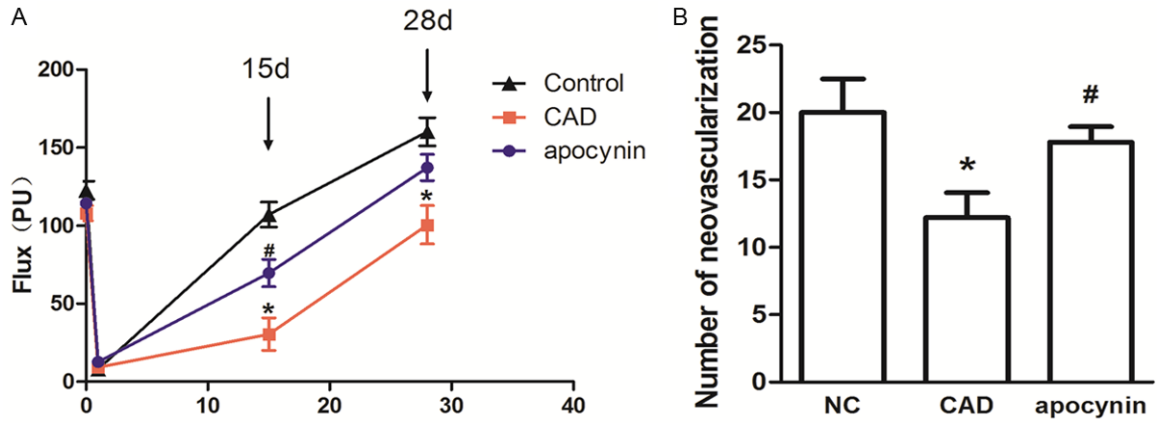

Figure 4. The blood perfusion in rat hind limb ischemia model of two groups. A. The blood perfusion in rats transplanted with CAD-EPCs indicated poorer perfusion compared with those rats transplanted with control-EPCs at day 15 and 28 (100.28 PU versus 27.9 PU and 153.6 PU versus 110.6 PU), n=10, 10, *P<0.05. While EPCs treated with apocynin and transplanted to a rat hind limb ischemia model showed a restored perfusion vs CAD group at day 15 (70 PU versus 30.4 PU), n=10, 10, #P<0.05, but not at day 28. B. Bar graph summarizing the vascular engraftment by EPCs. It demonstrated a decreased number (20 vs 12.2/mm^2) of DiI-labeled, red fluorescent EPC-derived vasculature compared to control groups at day 28, *P<0.05. But EPCs treated with apocynin and transplanted to a rat hind limb ischemia model resulted in a restored vascular engraftment vs CAD group (17.8 vs 12.2/mm^2), #P<0.05.

sion was performed at day 15 and 28 by Laser Doppler Flowmetry PeriFlux 5000 as described above. One of the output parameters perfusion unit (PU) was recorded. The blood flow in rats transplanted with CAD-EPCs indicated poorer perfusion compared with those rats transplanted with control-EPCs at day 15 and 28 (100.28 PU versus 27.9 PU and 153.6 PU versus 110.6 PU) (P<0.05) (**Figure 4A**). Transplanted EPCs marked with DiI (1,1'-dioctadecyl-3,3,3',3'-tetramethylindocarbocyanine perchlorate) were identified in tissue sections using red fluorescence. In contrast, the vasculature, stained using FITC, was identified using green fluorescence in the same tissue sections. Rats transplanted with CAD-EPCs demonstrated a decreased number (20 vs 12.2/mm^2) (P<0.05) of DiI-labeled, red fluorescent EPC-derived vasculature compared to control groups at day 28 (**Figures 4B**, **5**).

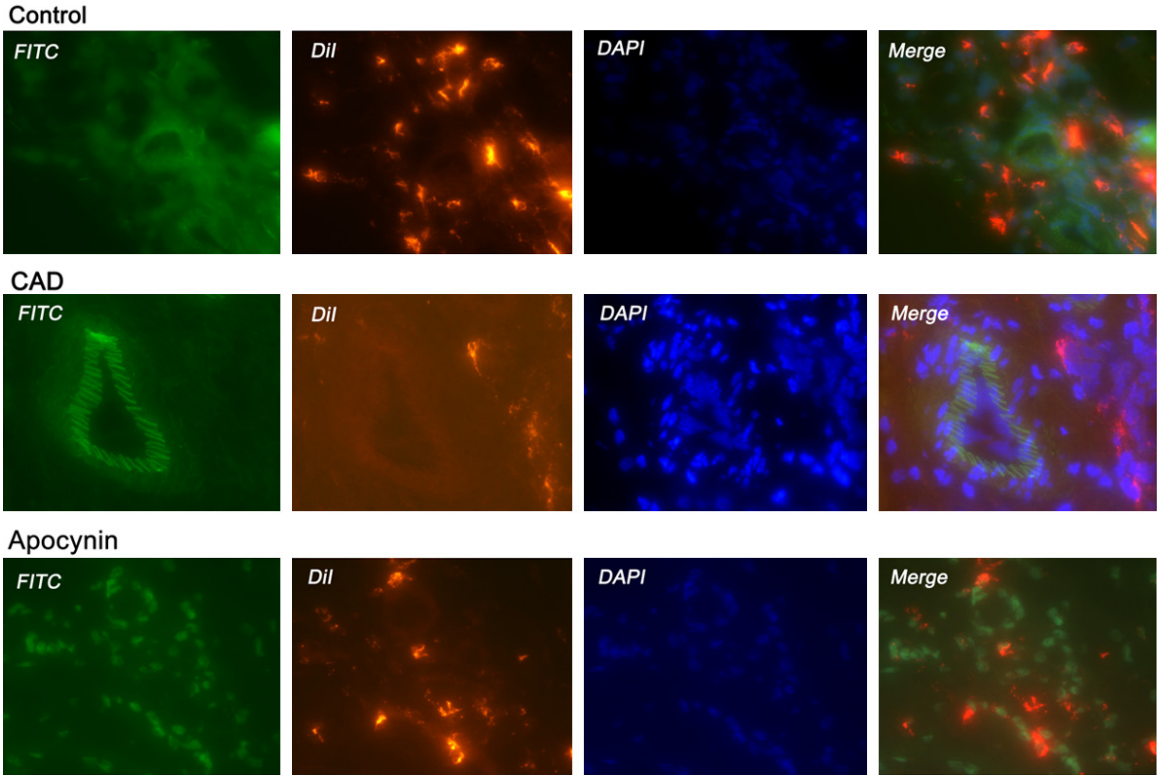

Figure 5. Immunohistochemistry image of vascular engraftment by EPCs. Rats transplanted with CAD-EPCs showed a low degree of vascular incorporation, while rats transplanted with CAD-EPCs which were treated with apocynin resulted in a restored vascular engraftment vs CAD group.

NADPH oxidase inhibition restores the generation of ROS and MDA and the in vivo angiogenesis capacity in EPCs from CAD subjects

Antioxidant NAC (3 mmol/L), apocynin (100 μmol/L) and subunit siRNA (50 nM) were used to inhibit the NADPH oxidase activation. First, subunit $p47^{phox}$, $gp91^{phox}$, Nox4 protein expression levels were reduced significantly by siRNA treatment, compared to the non-silenced group (**Figure 6A**). Either siRNA silencing of the NADPH oxidase subunit or inhibition by NAC and apocynin resulted in a markedly reduced NADPH oxidase activity and ROS generation in EPCs from CAD individuals (**Figure 6B**, **6C**). However, siRNA silencing did not decrease the MDA concentration while NAC and apocynin do reduced the concentration of MDA (**Figure 6D**).

In addition, inhibition of NADPH oxidase by apocynin partially reversed the blood perfusion at 15 d (70 PU versus 30.4 PU) and the number of neovascularization (17.8 vs 12.2/mm^2) compared to CAD group (**Figures 4** and **5**), which suggesting a critical role of NADPH oxidase activation in vivo angiogenesis capacity of EPCs.

The role of PKC in the activation of NADPH oxidase in EPCs from CAD subjects

We first examined the phosphorylation of PKCα, PKCβ1, PKCβ2 in CAD-EPCs and determined that PKCα and PKCβ2 phosphorylation were significantly enhanced in CAD-EPCs compared to the normal control group, but no significant changes were observed in PKCβ1 ($P<0.05$) (**Figure 7**). Next, GÖ6983 (catalog number G1918, Sigma) was used to inhibit the total activity of PKC. CAD-EPCs that without treated with the inhibitors were used as the control group. After PKC inhibition, both NADPH oxidase activity and ROS generation were reduced in EPCs from CAD ($P<0.05$) (**Figure 8A**). Furthermore, the expression of subunit $p22^{phox}$, $p47^{phox}$, gp91 and Nox4 were decreased by PKC inhibition significantly ($P<0.05$) (**Figure 8B**).

Discussion

Many studies have demonstrated that a variety of risk factors, including oxidative stress, may play different roles in stable coronary artery disease and ACS. CAD differs from ACS in terms

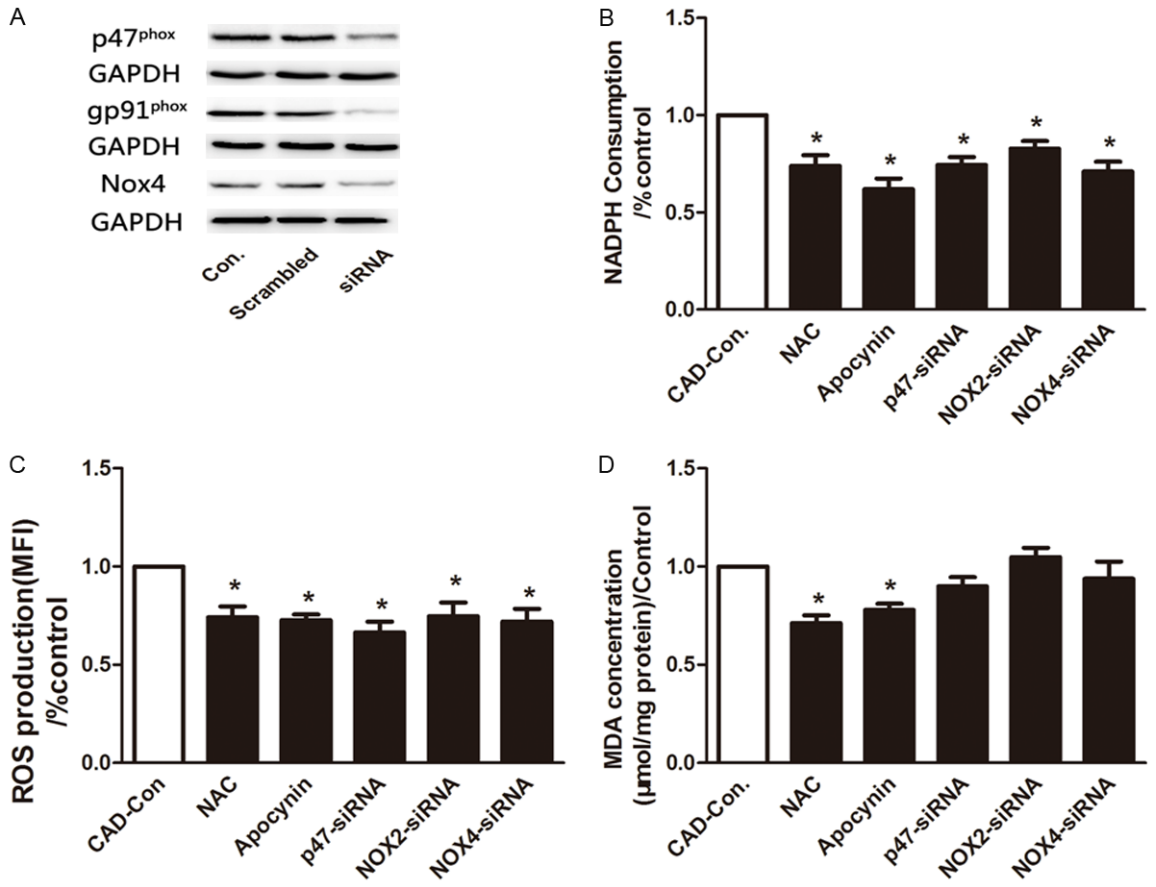

Figure 6. NADPH oxidase inhibition restores the generation of ROS and MDA. A. $p47^{phox}$, $gp91^{phox}$, Nox4 siRNA knockdown (KD). Western blot confirms that $p47^{phox}$, $gp91^{phox}$, Nox4 expression levels were reduced by approximately 60%, 85% and 65% following siRNA treatment. B. Relative NADPH activity 24 h after $p47^{phox}$, $gp91^{phox}$, Nox4 KD and inhibitors. Either siRNA silencing or inhibition by NAC and apocynin resulted in a markedly reduced NADPH oxidase activity in EPCs from CAD individuals, $^*P<0.05$. C. ROS production were also significantly decreased in CAD-EPCs pretreated with NAC, apocynin and siRNA silencing compared with CAD-EPCs without intervention, $^*P<0.05$. D. Relative MDA concentration 24 h after $p47^{phox}$, $gp91^{phox}$, Nox4 KD and inhibitors. siRNA silencing did not decrease the MDA concentration while NAC and apocynin do reduced the concentration of MDA, $^*P<0.05$.

of the release of chemoattractants and subsequent bone-marrow cell mobilization [12]. The number and function of circulating EPCs in stable CAD might more appropriately to represent the individual's capacity for endothelial repair. Thus, the current study will mainly focus on the effect of oxidative stress and the role of NADPH oxidase in EPCs with stable coronary artery disease.

It is widely established that oxidative stress plays a pivotal role in the development and pathogenesis of CAD and its complications [13]. Several studies have demonstrated that oxidative stress can result in the development of cardiovascular diseases by reducing the number of EPCs and impairing EPCs function [14]. Among these factors, NADPH oxidase plays an essential role [15]. Our results showed in EPCs isolated from CAD patients, NADPH oxidase activity, ROS and MDA levels were significantly increased, which indicated high oxidative stress levels in EPCs from CAD patients, and was consistent with previous studies. In fact, there have been many studies that have shown NADPH oxidase is the main regulatory enzyme of ROS, which can be used as an indicator of oxidative stress. Several potential sources of ROS have been implicated in endothelial physiology and pathophysiology, including the mitochondrial electron transport chain, xanthine oxidase, cytochrome P-450 enzyme, uncoupled nitric oxide synthase (NOS) and NADPH oxidase [16]. Our study showed that in

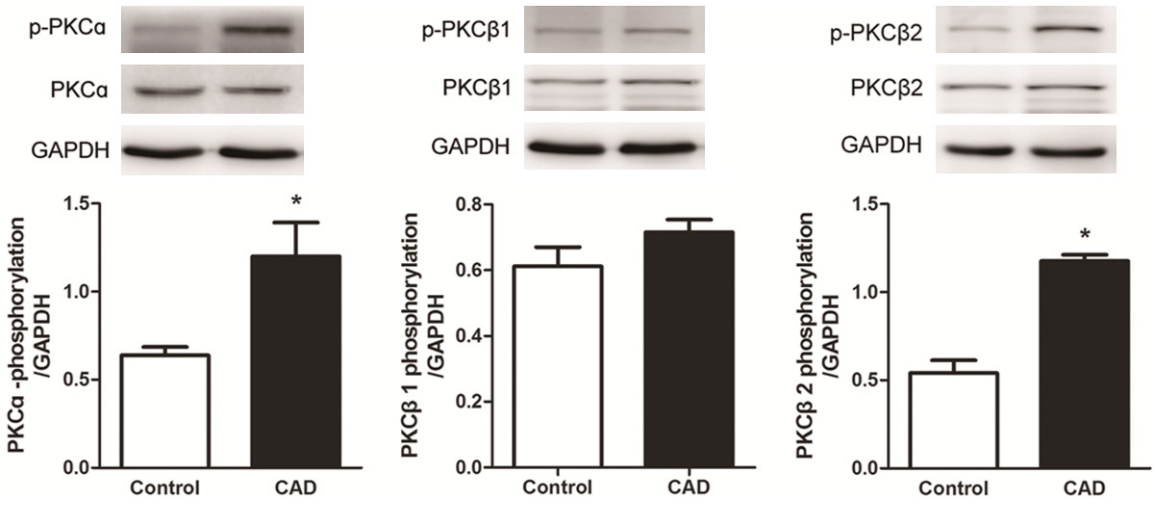

Figure 7. The phosphorylation of PKC subunits. PKCα/β2 phosphorylation were significantly up-regulated in CAD-EPCs vs control group, but no significant changes were observed in PKCβ1, n=12, 14, *P<0.05.

EPCs from CAD, ROS was primarily derived from NADPH oxidase and may partially correlate with endothelial nitric oxide synthase uncoupling, which indicated that the high levels of oxidative stress in CAD is indeed closely interrelated with NADPH oxidase activation.

NADPH oxidase includes five sub-fractions, which are membrane components gp91^{phox} (Nox2) and p22^{phox}, p47^{phox}, p67^{phox} and Rac are cytoplasmic components [17]. Their distribution is highly tissue-specific, different members of the Nox family have different activation mechanisms [18]. However, in CAD-EPCs, the precise pathophysiological function of each subunit and the activation mechanism remains unknown. Nox2 and Nox4 have been identified in diabetes as the predominant catalytic component of endothelial NADPH oxidase, and p47^{phox} plays an important role in regulating the activity of NADPH oxidase [19]. From our results we can infer that the subunit p22^{phox}, p47^{phox} and Nox2/4 may participate in NADPH oxidase activation, which may activated via membrane translocation of p47^{phox} and binding to Nox2 or Nox4 subunit. Immunoprecipitation detection showed small quantities of p47^{phox}-Nox4 conjugates, but no p47^{phox}-Nox2 conjugates were found (shown in Supplementary Figure 4). However, we need to do much deeper work to further validate this process here. Furthermore, in the cardiovascular system, Nox2 were mainly expressed in endothelial cells, cardiomyocytes, fibroblasts, and some of the VSMCs, Nox4 were mainly expressed in endothelial cells, VSMCs, cardiomyocytes and fibroblasts, we cannot rule out the possibility of p47^{phox} binding to Nox2 or Nox4 subunit. Nevertheless, one thing we can be sure that p47^{phox} plays a crucial role in regulating the activity of NADPH oxidase in CAD.

EPCs play pivotal roles in neovascularization and re-endothelialization in response to tissue ischemia and endothelial injury [20]. Several studies have shown that oxidative stress damages this functions of EPCs [21], however, the precise mechanism for this phenomenon is still unknown. We hypothesized that in CAD, the impaired vasculogenic capacity of EPCs is associated with an activation of NADPH oxidase. The present study showed that the in vivo angiogenesis capacity of EPCs from CAD subjects is severely impaired. Furthermore, when NADPH oxidase was inhibited by apocynin, the angiogenesis capacity of the CAD-EPCs was restored, suggesting a critical role of NADPH oxidase activation in the angiogenesis capacity. Although this has been demonstrated in diabetic EPCs, Sajoscha et al. reported that the in vivo re-endothelialization capacity of EPCs derived from individuals with diabetes mellitus was severely impaired by increased NADPH oxidase and reduced NO bioavailability. This study reports the first description of this phenomenon in EPCs from CAD, thus the NADPH oxidase system represents a promising target for correcting vasculogenic dysfunction in CAD-EPCs. However, apocynin can not reversed the blood

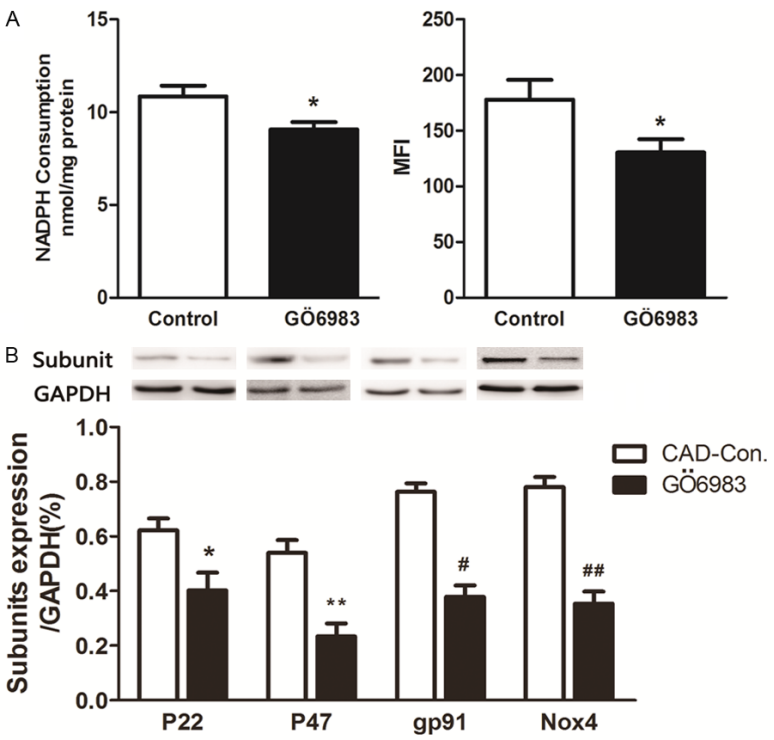

Figure 8. Effect of GÖ6983 on NADPH oxidase activity, ROS and the expression of NADPH oxidase subunits. A. CAD-EPCs were incubated in GÖ6983 for 30 min, CAD-EPCs that without treated with the inhibitors were used as control, both NADPH oxidase activity and ROS generation were reduced after PKC inhibition, n=10, 10, *P<0.05. B. Western blotting showed the expression of subunit $p22^{phox}$, $p47^{phox}$, $gp91^{phox}$ and Nox4 were decreased by GÖ6983 vs CAD control, n=8, 8, *,#P<0.05, **,##P<0.05.

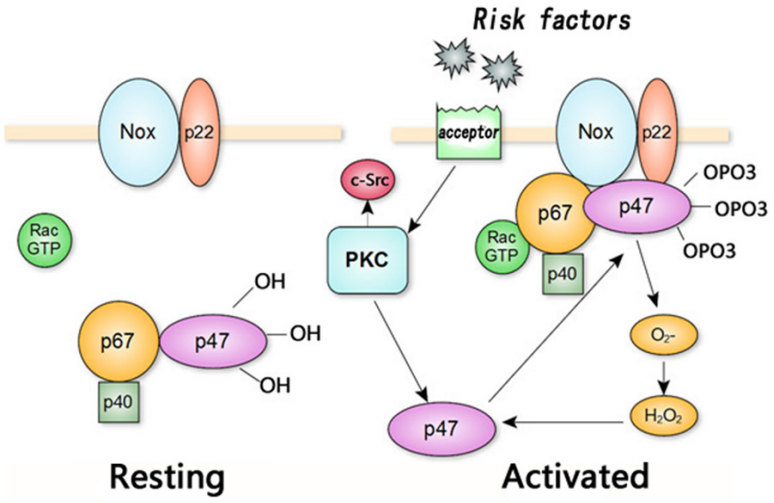

Figure 9. Possible processes of PKC mediated NADPH oxidase activation in EPCs.

perfusion at 28 d (137.2 PU versus 100.53 PU), P>0.05. Apocynin, which can inhibits NADPH oxidase activity [22], although this inhibition may be non-specific [23], but studies have proposed that apocynin is not an inhibitor of vascular NADPH oxidases, but an antioxidant [24], which imply that apocynin may inhibit the activity of NADPH oxidase through other mechanisms such as downstream pathways after NADPH oxidase activation. Furthermore, the effects of apocynin in transplanted EPCs were transient. Overall, our study provides a therapeutic approach to improve EPC function based on the inhibition of specific ROS generating enzymes-NADPH oxidases.

In stable coronary artery disease, various cardiovascular risk factors, including high cholesterol, hyperglycemia, smoking, hypoxia, etc. are all likely to lead to activation of NADPH oxidase. However, it can be activated by multiple signaling pathways and has many influencing factors, therefore it's very difficult to study in vivo. Protein kinase C activation is an important component of multiple vascular disease processes [25]. The phosphorylation of NADPH oxidase subunits may be associated with PKC activation caused by risk factors. It has been reported that in diabetes, PKC-mediated activation of small GTP binding to Rac1 directly contribute to the activation of NADPH oxidase, in which PKCβ play an important role. Sachin A. Gupte reported that peroxide generation by $p47^{phox}$-src activation of Nox2 has a key role in PKC-induced arterial smooth muscle contraction [26]. At present, most researchers focus on the mechanism of NADPH oxidase activation induced by AngII, and reported that the first

phase of Ang II-stimulated ROS production is dependent on protein kinase C activation [27]. In fact, there are a number of other studies have also pointed out that PKC plays an important role in the activation of NADPH oxidase. Monocytes mainly expressed PKCα, PKCβ1 and PKCβ2. In addition to the effects of PKCα/β activity on NADPH oxidase, the latest study also found that other PKC isozymes may also play a regulatory role in NADPH oxidase activation, such as PKCδ is also involved in controlling the phosphorylation and regulating the translocation of $p47^{phox}$ and $p67^{phox}$, PKCζ inhibitor can block the phosphorylation of $p47^{phox}$ and binding to $gp91^{phox}$ which induced by TNF-α. However, the relationship between NADPH oxidase activation and PKC stimulation in CAD-EPCs remains poorly understood. Our results indicated that PKCα/β2 phosphorylation was significantly enhanced in CAD-EPCs, and NADPH oxidase activity and ROS generation were reduced after PKC inhibition, suggesting the critical role of PKC in the activation of NADPH oxidase in CAD. Moreover, the expression levels of NADPH oxidase subunit has also been proved that was positively correlated with PKC activity. Although NADPH oxidase activation can through several ways, PKCα/β2 signaling pathway must be one of the mechanisms. Thus, if we can identify the upstream targets that inhibit NADPH oxidase activation, then we might be able to improve EPC function for the treatment of coronary heart disease.

In conclusion, we found that NADPH oxidase-mediated oxidative stress might be activated by one of the mechanisms PKCα/β2 signaling pathway and NADPH oxidase activation plays an important role in EPCs from CAD (**Figure 9**). This study provides evidence for a therapeutic approach to CAD based on the inhibition of specific ROS generating enzymes-NADPH oxidase, particularly the specific inhibition of activation-related subunits.

Acknowledgements

We thank the Biomedical Research Center in Sir Run Run Shaw Hospital, College of Medicine, Zhejiang University for the use of equipment. This work was supported by the National Natural Science Foundation of China (Grants 81070163), Zhejiang Provincial Medical and Health Science and Technology Plan (No. 2015KYB206) and Zhejiang Provincial Traditional Chinese Medical Technology Plan (No. 2016ZB072). We are grateful for the grant support from professor Fu. Guosheng and Weng shaoxiang for many valuable discussions and thoughtful critique of the manuscript. We also wish to thank Stephanie Jerman for help with the manuscript.

Disclosure of conflict of interest

None.

Address correspondence to: Dr. Guosheng Fu, Department of Cardiology, Sir Run Run Shaw Hospital, 3 East Qingchun Road, Hangzhou 310016, Zhejiang Province, China. Tel: +86 571 86006241; E-mail: fugssrrsh@163.com

References

[1] Shantsila E, Watson T, Lip GY. Endothelial progenitor cells in cardiovascular disorders. J Am Coll Cardiol 2007; 49: 741-52.

[2] Werner N, Wassmann S, Ahlers P, Schiegl T, Kosiol S, Link A, Walenta K, Nickenig G. Endothelial progenitor cells correlate with endothelial function in patients with coronary artery disease. Basic Res Cardiol 2007; 102: 565-71.

[3] Enseleit F, Sudano I, Periat D, Winnik S, Wolfrum M, Flammer AJ, Fröhlich GM, Kaiser P, Hirt A, Haile SR, Krasniqi N, Matter CM, Uhlenhut K, Högger P, Neidhart M, Lüscher TF, Ruschitzka F, Noll G. Effects of Pycnogenol on endothelial function in patients with stable coronary artery disease: a double-blind, randomized, placebo-controlled, cross-over study. Eur Heart J 2012; 33: 1589-97.

[4] Bilinska M, Wolszakiewicz J, Duda M, Janas J, Beresewicz A, Piotrowicz R. Antioxidative activity of sulodexide, a glycosaminoglycan, in patients with stable coronary artery disease: a pilot study. Med Sci Monit 2009; 15: CR618-23.

[5] Sorrentino SA, Bahlmann FH, Besler C, Muller M, Schulz S, Kirchhoff N, Doerries C, Horváth T, Limbourg A, Limbourg F, Fliser D, Haller H, Drexler H, Landmesser U. Oxidant stress impairs in vivo reendothelialization capacity of endothelial progenitor cells from patients with type 2 diabetes mellitus: restoration by the peroxisome proliferator-activated receptor-gamma agonist rosiglitazone. Circulation 2007; 116: 163-73.

[6] Tan Y, Li X, Prabhu SD, Brittian KR, Chen Q, Yin X, McClain CJ, Zhou Z, Cai L. Angiotensin II plays a critical role in alcohol-induced cardiac nitrative damage, cell death, remodeling, and

cardiomyopathy in a protein kinase C/nicotinamide adenine dinucleotide phosphate oxidase-dependent manner. J Am Coll Cardiol 2012; 59: 1477-86.
[7] Punshon G, Vara DS, Sales KM, Seifalian AM. A novel method for the extraction and culture of progenitor stem cells from human peripheral blood for use in regenerative medicine. Biotechnol Appl Biochem 2011; 58: 328-34.
[8] Bao XM, Wu CF, Lu GP. Atorvastatin inhibits homocysteine-induced oxidative stress and apoptosis in endothelial progenitor cells involving Nox4 and p38MAPK. Atherosclerosis 2010; 210: 114-21.
[9] Ebrahimian TG, Heymes C, You D, Blanc-Brude O, Mees B, Waeckel L, Duriez M, Vilar J, Brandes RP, Levy BI, Shah AM, Silvestre JS. NADPH oxidase-derived overproduction of reactive oxygen species impairs postischemic neovascularization in mice with type 1 diabetes. Am J Pathol 2006; 169: 719-28.
[10] Zhang JK, Yang L, Meng GL, Fan J, Chen JZ, He QZ, Chen S, Fan JZ, Luo ZJ, Liu J. Protective effect of tetrahydroxystilbene glucoside against hydrogen peroxide-induced dysfunction and oxidative stress in osteoblastic MC3T3-E1 cells. Eur J Pharmacol 2012; 689: 31-7.
[11] Borchi E, Parri M, Papucci L, Becatti M, Nassi N, Nassi P, Nediani C. Role of NADPH oxidase in H9c2 cardiac muscle cells exposed to simulated ischaemia-reperfusion. J Cell Mol Med 2009; 13: 2724-35.
[12] Bakogiannis C, Tousoulis D, Androulakis E, Briasoulis A, Papageorgiou N, Vogiatzi G, Kampoli AM, Charakida M, Siasos G, Latsios G, Antoniades C, Stefanadis C. Circulating endothelial progenitor cells as biomarkers for prediction of cardiovascular outcomes. Curr Med Chem 2012; 19: 2597-604.
[13] Lin CP, Lin FY, Huang PH, Chen YL, Chen WC, Chen HY, Huang YC, Liao WL, Huang HC, Liu PL, Chen YH. Endothelial progenitor cell dysfunction in cardiovascular diseases: role of reactive oxygen species and inflammation. Biomed Res Int 2013; 2013: 845037.
[14] De Winter RJ, Klomp M. Understanding the role of endothelial progenitor cells in cardiovascular disease, coronary artery lesion progression, and in-stent restenosis. JACC Cardiovasc Interv 2010; 3: 87-9.
[15] Jarajapu YP, Caballero S, Verma A, Nakagawa T, Lo MC, Li Q, Grant MB. Blockade of NADPH oxidase restores vasoreparative function in diabetic CD34+ cells. Invest Ophthalmol Vis Sci 2011; 52: 5093-104.
[16] Satoh M, Fujimoto S, Haruna Y, Arakawa S, Horike H, Komai N, Sasaki T, Tsujioka K, Makino H, Kashihara N. NAD(P)H oxidase and uncoupled nitric oxide synthase are major sources of glomerular superoxide in rats with experimental diabetic nephropathy. Am J Physiol Renal Physiol 2005; 288: F1144-52.
[17] Li H, Liu Q, Wang N, Xu J. Correlation of different NADPH oxidase homologues with late endothelial progenitor cell senescence induced by angiotensin II: effect of telmisartan. Intern Med 2011; 50: 1631-42.
[18] Lassegue B, Clempus RE. Vascular NAD(P)H oxidases: specific features, expression, and regulation. Am J Physiol Regul Integr Comp Physiol 2003; 285: R277-97.
[19] Haddad P, Dussault S, Groleau J, Turgeon J, Michaud SE, Menard C, Perez G, Maingrette F, Rivard A. Nox2-containing NADPH oxidase deficiency confers protection from hindlimb ischemia in conditions of increased oxidative stress. Arterioscler Thromb Vasc Biol 2009; 29: 1522-8.
[20] Wojakowski W, Kucia M, Kazmierski M, Ratajczak MZ, Tendera M. Circulating progenitor cells in stable coronary heart disease and acute coronary syndromes: relevant reparatory mechanism? Heart 2008; 94: 27-33.
[21] Tousoulis D, Kampoli AM, Stefanadis C. Diabetes mellitus and vascular endothelial dysfunction: current perspectives. Curr Vasc Pharmacol 2012; 10: 19-32.
[22] Li M, Liu Z, Zhuan L, Wang T, Guo S, Wang S, Liu J, Ye Z. Effects of apocynin on oxidative stress and expression of apoptosis-related genes in testes of diabetic rats. Mol Med Rep 2013; 7: 47-52.
[23] Senejoux F, Girard-Thernier C, Berthelot A, Bevalot F, Demougeot C. New insights into the mechanisms of the vasorelaxant effects of apocynin in rat thoracic aorta. Fundam Clin Pharmacol 2013; 27: 262-70.
[24] Heumuller S, Wind S, Barbosa-Sicard E, Schmidt HH, Busse R, Schroder K, Brandes RP. Apocynin is not an inhibitor of vascular NADPH oxidases but an antioxidant. Hypertension 2008; 51: 211-7.
[25] Barman SA. Vasoconstrictor effect of endothelin-1 on hypertensive pulmonary arterial smooth muscle involves Rho-kinase and protein kinase C. Am J Physiol Lung Cell Mol Physiol 2007; 293: L472-9.
[26] Gupte SA, Kaminski PM, George S, Kouznestova L, Olson SC, Mathew R, Hintze TH, Wolin MS. Peroxide generation by p47phox-Src activation of Nox2 has a key role in protein kinase C-induced arterial smooth muscle contraction. Am J Physiol Heart Circ Physiol 2009; 296: H1048-57.
[27] Seshiah PN, Weber DS, Rocic P, Valppu L, Taniyama Y, Griendling KK. Angiotensin II stimulation of NAD(P)H oxidase activity: upstream mediators. Circ Res 2002; 91: 406-13.

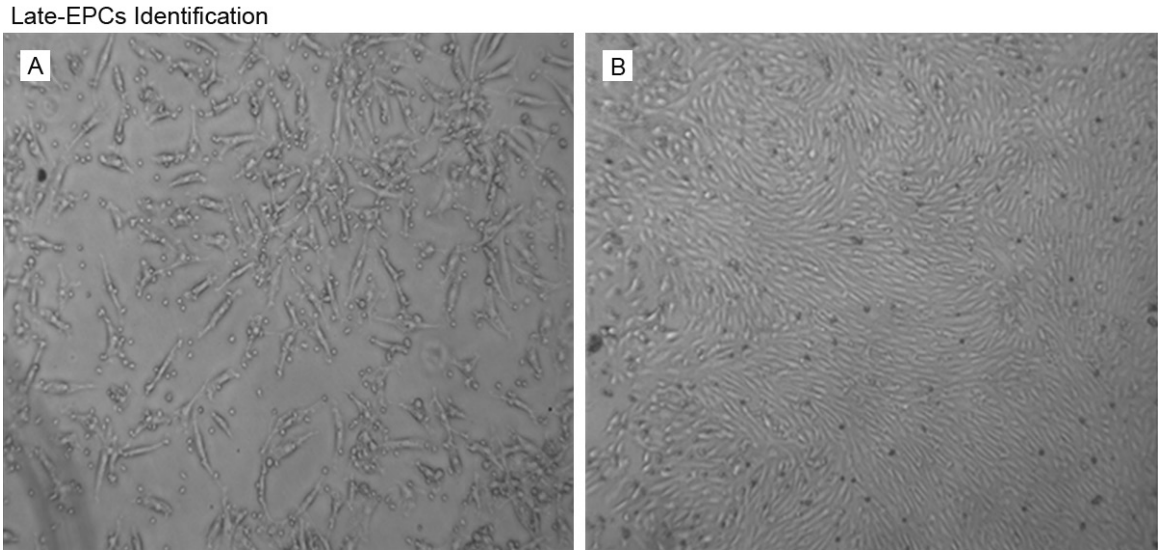

Supplementary Figure 1. A. Early EPC: Non-adherent cells were cultured for 7 days after re-seed plate and exhibited spindle-shaped endothelial-like cells under an inverted microscope (200×). B. Late EPC: Cell culture to 14-28 days, L-EPC grown to confluence showing a cobblestone-like monolayer (200×).

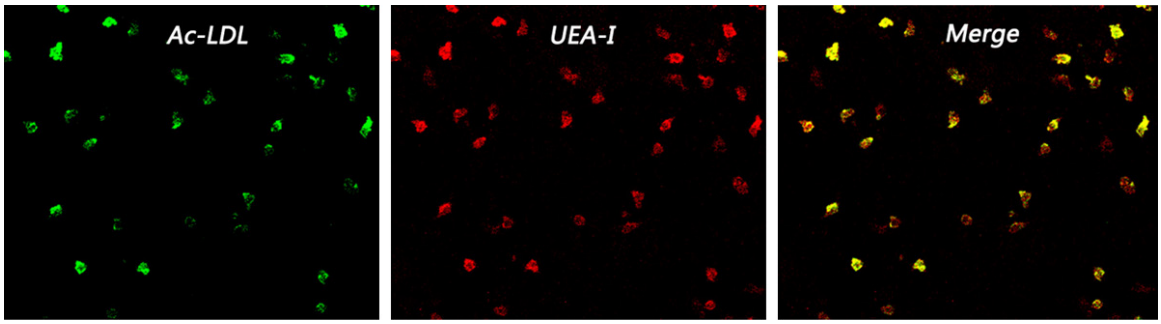

Supplementary Figure 2. Mononuclear cells were cultured for 2-4 weeks, and adherent cells lectin binding (green, exciting wave-length 477 nm) and DiI-LDL uptake (red, exciting wave-length 543 nm) were assessed under a laser scanning confocal microscope. Double positive cells appearing yellow in the overlay were identified as differentiating EPCs (400×).

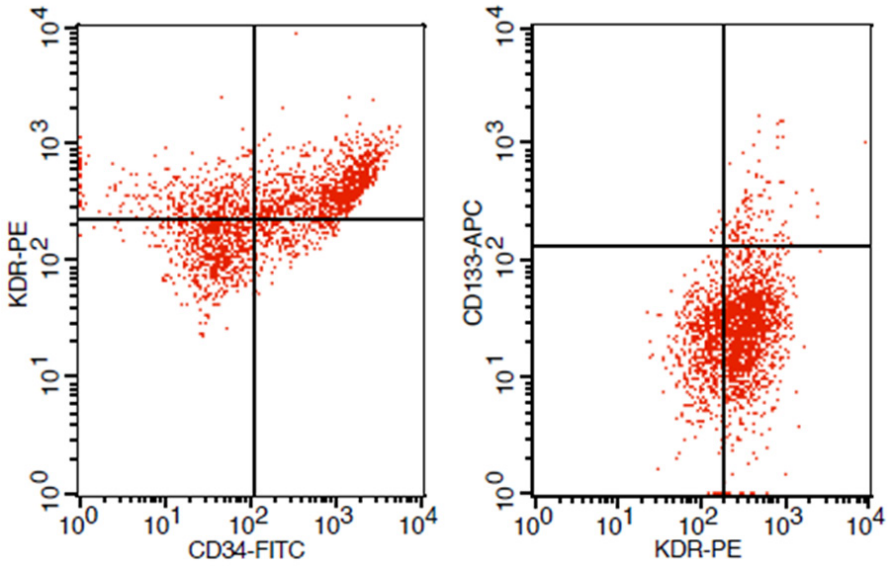

Supplementary Figure 3. Flow cytometry identified L-EPC surface antibody: VEGFR-2 (KDR, 78.4 ± 7.6%), CD34 (28.7 ± 6.5%), CD133 (ie, AC133, 17.4 ± 5.6%).

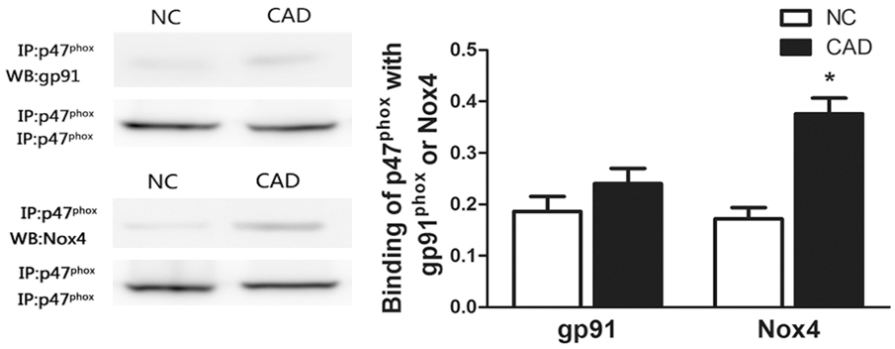

Supplementary Figure 4. Immunoprecipitation detection of $p47^{phox}$ combined with Nox2/4 within EPCs. Immune complex formation of $p47^{phox}$-Nox4 conjugates were increased in CAD group compared to normal control group, n=10, 10, $^*P<0.05$. However, no $p47^{phox}$-Nox2 conjugates were found.